Photodissociation of Water Dimer at 205 nm†

Masahiro Kawasaki,* Akihiro Sugita, and Christopher Ramos

Department of Molecular Engineering and School of Global Environmental Studies, Kyoto University, Kyoto 615-8510, Japan

Yutaka Matsumi

Solar Terrestrial Environment Laboratory, Nagoya University, Toyokawa 442-8507, Japan

Hiroto Tachikawa

Department of Molecular Chemistry, Faculty of Engineering, Hokkaido University, Sapporo 060-8501, Japan

Received: March 15, 2004; In Final Form: May 20, 2004

A deuterated water dimer, $(D_2O)_2$, absorbs a photon at 205 nm releasing a fragment D atom. The negative angular anisotropy parameters are observed experimentally with photofragment imaging spectroscopy. In this dissociation, one of the translational energy distributions obtained for the fragment D atoms peaks at around 1 kcal mol^{-1}, which is much smaller than the maximum available energy, 16.2 kcal mol^{-1}. These results suggest an energy loss process of the fragment D atom, which is induced by a collision with the oxygen atom in the dimer before it leaves the parent molecule. A direct ab initio trajectory calculation for the internal collision process of the D atom in the dimer has been performed. The obtained energy loss is in good agreement with the present experimental results.

Introduction

A water monomer has a UV absorption band in the vacuum UV region below 185 nm. The absorption cross section of H_2O at $\lambda > 200$ nm is as small as 10^{-23} cm^2 at 200 nm.[1] The corresponding cross section of D_2O is 2 orders of magnitude smaller.[2] Thus, the photochemistry of the water monomer is important only in the vacuum UV region. As is known for water ice, the higher clusters have blue-shifted photoabsorption in the vacuum UV region. Gerber and co-workers performed theoretical calculations to predict the UV absorption bands of water clusters.[3,4] The main absorption peak shifts toward blue as the number of water molecules in the clusters increases. They found that only the dimer should have an appreciable absorption cross section around 10^{-20} cm^2 to the red of 190 nm, because the dimer is a unique case in which one water molecule is donating a hydrogen bond but not receiving one.[3] The red-shifted absorption is attributed to the low excitation energy of the hydrogen bond donor water molecule. All other water cyclic clusters exhibit a blue shift in the UV absorption bands because each water molecule is equally considered as a hydrogen bond donor as well as an acceptor.[3,4] The ground state geometry computed for the water dimer places the O−O distance at 2.98 Å, the hydrogen bond acceptor angle at 30°, and the hydrogen bond donor angle at 56°.[5] In the ground state of the D_2O dimer, the hydrogen bond energy is reported to be 3.40−3.66 kcal mol^{-1}. Since water molecules are easily clustered under the conditions of a low-temperature molecular beam, experimental difficulty concerning the photochemistry of the dimer arises from the coexistence of various sized clusters in the molecular beam. However, the water dimer can be selectively excited at $\lambda > 200$ nm through its characteristic absorption to the red of the monomer and the higher clusters. We present here an examination of the photodissociation dynamics of the water dimer with photofragment spectroscopy to investigate the energy and angular distributions of the photofragments, which has been introduced by Bersohn, Zare, Wilson, and their co-workers.[6−8]

Experimental Section

The velocity ion imaging experiments are performed with an imaging apparatus.[9,10] A brief description of the apparatus follows.[11] The molecular beam is introduced into the time-of-flight apparatus via a pulsed valve with a nozzle diameter of 0.8 mm (General Valve). The backing pressure is 1100 Torr of Ar plus 25 Torr of D_2O at room temperature. Under this pressure condition, the higher clusters of water molecules are more populous than the monomer in the delayed part of the pulsed molecular beam. Once introduced into the chamber, the pulsed jet is skimmed and then photodissociated by a tunable UV light that is provided by tripling the 615 nm output of an Nd^{3+}:YAG pumped dye laser (Lambda Physik, SCANmate) with a BBO crystal of type I. Maximum power is achieved by using a 1:1 mixture of rhodamine 610 and 640 dyes. Although the 615 nm light becomes off-axis after a 1 m travel path, the 307.43 nm light (1 mJ pulse^{-1}) is not separated from the 205.09 nm laser light (0.2 mJ pulse^{-1}). We do not use a Pellin−Broca prism or a mirror because the 205 nm intensity is weakened by the optics. The two UV laser beams are introduced simultaneously into the interaction region with a lens ($f = 20$ cm) with their electric vector directions perpendicular to each other. The electric vector at 205.09 nm is perpendicular to the molecular beam axis while that at 307 nm is directed toward a microchannel plate detector (MCP). Although the 205 nm laser light is not separated from the 307 nm light in the present experiment, the 307 nm photon would not participate in the photodissociation processes because the focal point of the 307 nm laser is longer than that of the 205 nm laser by 2 cm. Because of this position difference in

† Part of the special issue "Richard Bersohn Memorial Issue".

* Corresponding author. E-mail: kawasaki@moleng.kyoto-u.ac.jp. Fax +81-75-383-2573.

10.1021/jp048857w CCC: $27.50
Published on Web 06/25/2004

the ion optics of the imaging spectrometer that is tuned for the focused 205 nm laser, the photoprocesses caused by the 307 nm photons would not effect the observed images. In addition, since the state of the water dimer photoprepared by 205 nm light is dissociative with a short lifetime, it cannot absorb the 307 nm photon. The observed images are due to photoprocesses by the 205 nm photons.

Under the one-color laser scheme at 205 nm, the parent molecules are photodissociated and photofragment D atoms are subsequently ionized by the (2 + 1) resonance-enhanced multiphoton ionization (REMPI) through the 3^2S or 3^2D levels. The (3 + 1) REMPI process could occur simultaneously, but its contribution would be small. The one-color REMPI method at this wavelength was first performed by Bersohn and coworkers.[12] We have tested this method with hydrogen sulfide, which has been extensively investigated. The product atom is recoiled by the photoelectron in the (2 + 1) multiphoton ionization process. This recoil energy, 0.028 kcal mol^{-1}, is taken into account in the analysis of the translational energy of the fragment D atoms. The laser wavelength is scanned over the Doppler profile of the D photofragment. The thus-produced ions are accelerated to the field free region of a time-of-flight mass spectrometer where they impinge on the MCP. Impact with the MCP in a given mass gate of the mass spectrum is monitored by imaging a phosphor screen via a CCD camera attached with a gated image intensifier (Hamamatsu Photonics). Time-of-flight mass spectral data are obtained by monitoring the MCP current. Observed images are back-projected by a method similar to that used in computerized tomography.[11] The angular anisotropy parameter, β, is obtained by a least-squares fit of the three-dimensional slice of the angular distribution function

$$I(\theta) = A\{1 + \sum \beta_{2n} P_{2n}(\cos \theta)\} \quad (1)$$

where $I(\theta)$ is the normalized angular distribution of the D atom photofragment. θ is the angle between the fragment velocity and the electric vector of the dissociation laser light. $P_{2n}(x)$ is the 2*n*th Legendre polynomial for *n*-photon dissociation.

In order to obtain the background images, multiphoton dissociation of water clusters is performed under the one-color laser scheme at 243 nm. Photofragment D atoms are subsequently ionized by the (2 + 1) REMPI at 243.07 nm through the 2^2S level. Coumarin 102 dye is used for the dye laser. With a Pellin−Broca prism, the fundamental laser light at 486 nm is eliminated.

Experimental Results

The REMPI signal intensity of the D atoms produced by the focused laser light at 205 nm was measured as a function of the delay time between the pulses of the dissociation laser and the molecular beam. The signal intensity peaked at 750 μs, while a typical delay time for photodissociation of isolated simple molecules is 500 μs for our apparatus. The long delay suggests that the D atoms come from the photodissociation of clusters and not monomers. The possible photodissociation of the monomer is eliminated. A typical photofragment image of the D atoms is presented in Figure 1A. The signal intensity decreases with increasing speed of the fragment and consists of two different distributions: a center ring component with angular anisotropy and an outer one without angular anisotropy.

The monomer absorption of D_2O starts at 183 nm, and the experimentally reported photodissociation cross section at 193 nm is low, 10^{-24} cm^2.[1,2] On the basis of the ab initio calculations by Harvey et al.,[3] Miller et al.,[4] and our group as will be described below, water clusters higher than the trimer have absorption at wavelengths shorter than 180 nm. Hence, it is reasonable to assume that (a) dimers in the water molecular beam are photodissociated at 205 nm by the one-photon dissociation process 2 and also (b) the higher clusters are photodissociated by the simultaneous multiphoton dissociation process 3

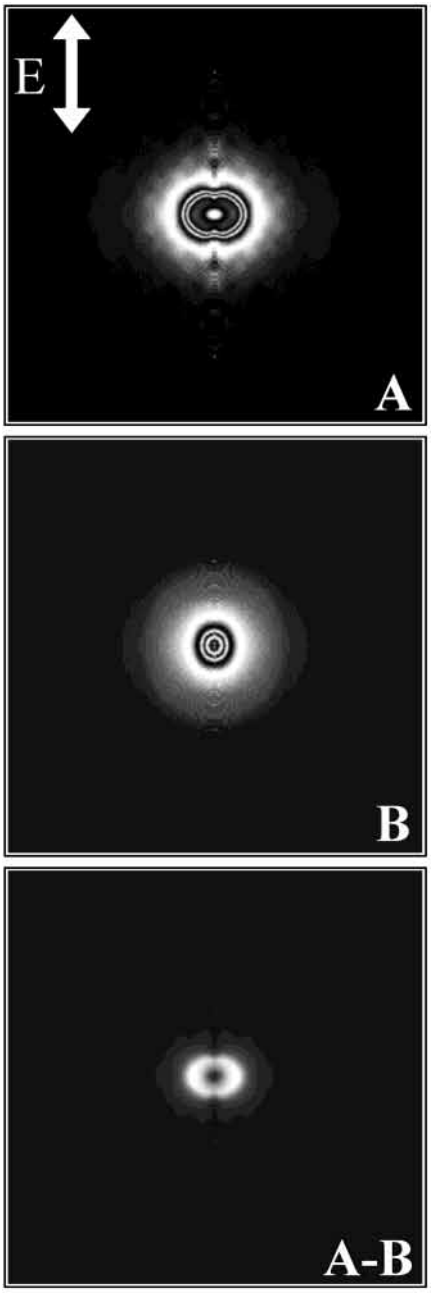

Figure 1. REMPI photofragment images of D atoms from the one- and multiphoton dissociation processes of dimers and clusters of D_2O by excitation at 205 nm (A) and the multiphoton dissociation process by excitation at 243 nm (B). Arrows show the directions of the electric vectors of 205 and 243 nm laser light. The difference image of panels A and B is shown in the bottom panel. The residual image corresponds to the contribution from the one-photon dissociation of $(D_2O)_2$ at 205 nm.

$$(D_2O)_2 + h\nu(205\ \text{nm}) \rightarrow (D_2O)_2^* \rightarrow D + OD + D_2O \quad (2)$$

$$(D_2O)_n + mh\nu(205\ \text{nm}) \rightarrow (D_2O)_n^* \rightarrow D + \text{fragments} \quad (3)$$

Since the nature of the electronic state of $(D_2O)_2^*$ is essentially the A^1B_1 state of the monomer, the angular distribu-

tion of the D atom photofragments should be anisotropic for the one-photon process 2. On the contrary, the angular distribution from the multiphoton process 3 of $(D_2O)_n$ is isotropic because the angles of fragmentation are, on the average, isotropic due to the combination of different structures of the clusters. This is ensured by the multiphoton dissociation at 243 nm as described below.

The image in Figure 1A consists of two different processes at 205 nm: one-photon dissociation of the dimer and multiphoton dissociation of the clusters, which are much more abundant than the dimer in the molecular beam. In order to extract the information about the one-photon dissociation from the overlapped image data, a simultaneous multiphoton dissociation of the water molecular beam was performed at 243 nm.

$$(D_2O)_n + mh\nu(243\text{ nm}) \rightarrow (D_2O)_n^* \rightarrow D + \text{fragments} \quad (4)$$

The one-photon transition at this wavelength is not in resonance with any electronic transitions of the monomer, dimer, and the higher clusters. The one-photon energy at 243 nm is smaller than the bond dissociation energy of the O−D bond by 3.5 kcal mol^{-1}. The simultaneous (coherent) two-photon excitation of the monomer H_2O at 240−250 nm was reported by Zhang et al.[13] The second Rydberg band, $C(^1B_1)-X(^1A_1)$, for the 3p−n(2p) transition appears at 125−143 nm. The photoprepared excited state, $C(^1B_1)$, is bound near the Franck−Condon region but is predissociated by the $B(^1A_1)$ and $A(^1B_1)$ states. A typical image of the D atoms produced by the photoexcitation at 243 nm is presented in Figure 1B. Its angular distribution is isotropic as expected for the cluster multiphoton dissociation. The angular anisotropy parameter β_2 is almost zero with slightly positive values up to 0.2, and the higher terms are not observed. The speed distribution is close to what is observed in the isotropic part of Figure 1A. Since the counter fragment works as a large bath for energy relaxation, the D atoms from the multiphoton dissociation of clusters are translationally relaxed.

The contribution of the cluster photodissociation (Figure 1B) is subtracted from Figure 1A. The bottom panel of Figure 1 shows the residual image that corresponds to the one-photon dissociation of the dimer at 205 nm. The angular anisotropy is clearly seen in this residual image. In the subtraction method we used two images at a 750 μs delay, which were observed at different wavelengths, 205 nm for signal and 243 nm for background. Even when the subtraction factor is changed by 15%, the residual image is essentially the same, especially in the narrow velocity region (0−3000 m s^{-1}), because the background image observed at 243 nm is isotropic in angular distribution and Maxwell−Boltzmann type in velocity distribution. In order to ensure that our subtraction method is appropriate, a residual image at a different delay time is tested, that is, a signal image at 205 nm and 500 μs delay and a background image at 243 nm and 750 μs delay. The residual image thus obtained looks useless. The velocity distributions obtained from the corresponding images of Figure 1 are shown in Figure 2. One notices that the velocity distribution peaks at 2300 m s^{-1} in the residual distribution. By back-projecting the residual image of Figure 1(A − B), the center-of-mass translational energy distribution and the angular anisotropy parameters are obtained and are shown in Figure 3. In this calculation, the OD radical is taken as the counter fragment. When a complex of OD + D_2O is taken as the counter fragment, the calculated translational energies increases only by 5%. The translational energy distribution peaks at around 1 kcal mol^{-1}. A contribution appears in the higher translational energy region. The angular

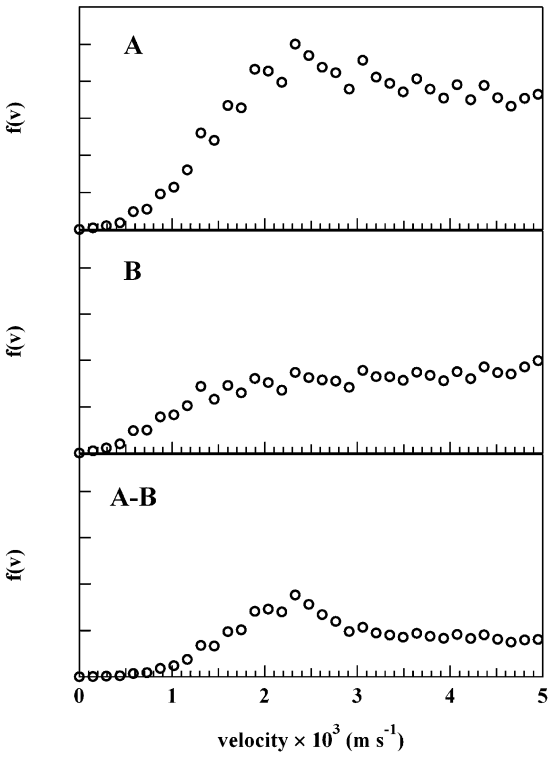

Figure 2. Velocity distributions of D atoms obtained from the corresponding images of Figure 1.

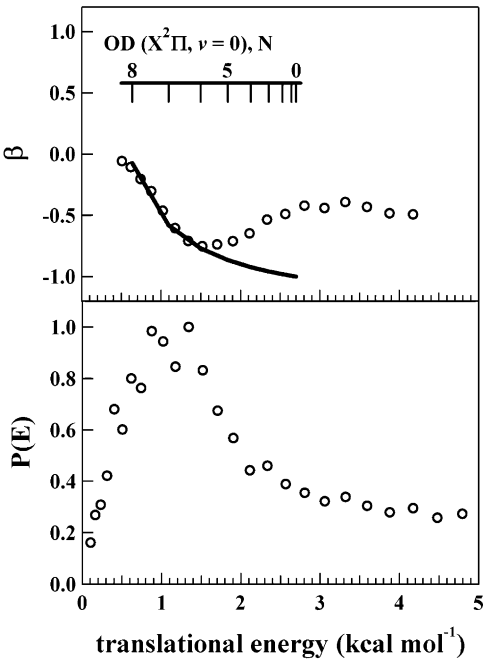

Figure 3. Angular anisotropy parameter and center-of-mass translational energy distributions of D atom photofragments from the one-photon dissociation process of $(D_2O)_2$ at 205 nm. The upper panel shows the angular anisotropy parameter distribution for β_2 of eq 1. The solid curve represents a simulated distribution according to eq 5 for various rotational levels of the OD fragments. R_c = 1.4 Å and E_{avl} = 2.7 kcal mol^{-1}. The lower panel shows the energy distribution obtained from the residual image A − B of Figure 1.

anisotropy parameters, β_2, first decrease from zero to −0.8 as the translational energy increases, then the β_2 values slightly increase from −0.8 to −0.5.

According to Plusquellic et al.[2] the D atom products from the photolysis of D_2O monomers at 193 nm are translationally hot. Thus, we believe that (a) the smaller energy component

can be attributed to the D photofragments with energy loss by collision processes and (b) the higher energy component to those without it. Since the higher energy component is strongly affected by the background isotropic image, we will not discuss it further and will focus on the smaller energy component. The energy of the O−D bond in water is 119.8 ± 0.05 kcal mol^{-1}, and taking the energy of the hydrogen bond to be 3.5 ± 0.1 kcal mol^{-1} the total energy required to remove the D atom participating in the hydrogen bond is 123.3 kcal mol^{-1}.[14] The energy injected into the system by one photon of 205.09 nm light is 139.4 kcal mol^{-1}. Subtracting the two energies leaves 16.2 kcal mol^{-1} for the fragments, however, the translational energy distribution of the slower fragments peaks at about 1 kcal mol^{-1}. The remaining 15 kcal mol^{-1} is likely transferred to the internal energy of OD and D_2O.

Theoretical Method

Electronic Excitation Energies of the Water Monomer and Clusters. The monomer photoabsorption of H_2O/D_2O starts at 188/183 nm with a cross section of 1×10^{-20} cm^2, respectively, and has its first maximum at 166 nm.[1] This is the Rydberg band of the 3s−n(2p) transition and the A^1B_1 state. At the B3LYP/6-311+G(d,p)//MP2/6-311++G(d,p) level, we calculate the first vertical excitation energies for water monomer, dimer, and cyclic clusters with the Gaussian 98 program:[15] 7.78 eV for H_2O, 7.05 eV for $(H_2O)_2$, 7.87 eV for $(H_2O)_3$, 7.98 eV for $(H_2O)_4$, 7.74 eV for $(H_2O)_5$, and 7.88 eV for $(H_2O)_6$. The structure of the water dimer $(H_2O)_2$ is fully optimized at the HF/6-311+G(d,p) and MP2/6-311++G(d,p) levels. The optimized structures and geometrical parameters are illustrated in Figure 4.

The dimer excitation energy is lowest among the monomer and clusters. A water dimer absorbs radiation by one of the water moieties, which has its energy levels lowered by the hydrogen bond interaction with the second water molecule. This is in good agreement with the results calculated by Harvey et al.[3] They reported that the dimer absorption band is red-shifted from the monomer absorption band, while the absorption maxima of the cyclic clusters are blue-shifted. In addition, they reported that the absorption tail of the dimer goes much further to the red than the vertical excitation energy position, due to the wings in the ground state vibrational wave function that extends into the valleys of the dissociative excited state potential in the 1.3−1.4 nm region of the OH bond lengths.

Second, to elucidate the stabilization mechanism in the electronically excited dimer of water, CAS(4,4)/6-311++G(d,p)//MP2/6-311++G(d,p) calculations are carried out for the monomer and dimer of water and methanol. The vertical excitation energies of H_2O and $(H_2O)_2$ are calculated to be 6.73 and 6.52 eV, respectively. The charge of the free hydrogen (non-hydrogen-bonding H atom) of the donor water molecule is negative (−0.88) in the first excited state. This result indicates that the electron transfer occurs from the orbital of the hydrogen bond to the free hydrogen atom of the donor molecule. This is the origin of the stabilization of the electronically excited dimer of water. In other words, the lower energy for the dimer is attributed to the high polarizability of the hydrogen bond donor water molecule in its electronically excited state because the excited state is stabilized by electron transfer from the hydrogen bond orbital to the hydrogen atom (not the hydrogen-bonded one) of the donor molecule. The same calculations are carried out for methanol and the methanol dimer where the free hydrogen is substituted by a methyl group. The monomer and dimer of methanol have excitation energies of 6.84 eV for CH_3OH and 7.12 eV for $(CH_3OH)_2$, indicating that the vertical excitation energy of the methanol dimer is blue-shifted from that of the methanol monomer. This is due to the fact that electron transfer cannot occur in the case of the methanol dimer, and the stabilization mechanism does not work.

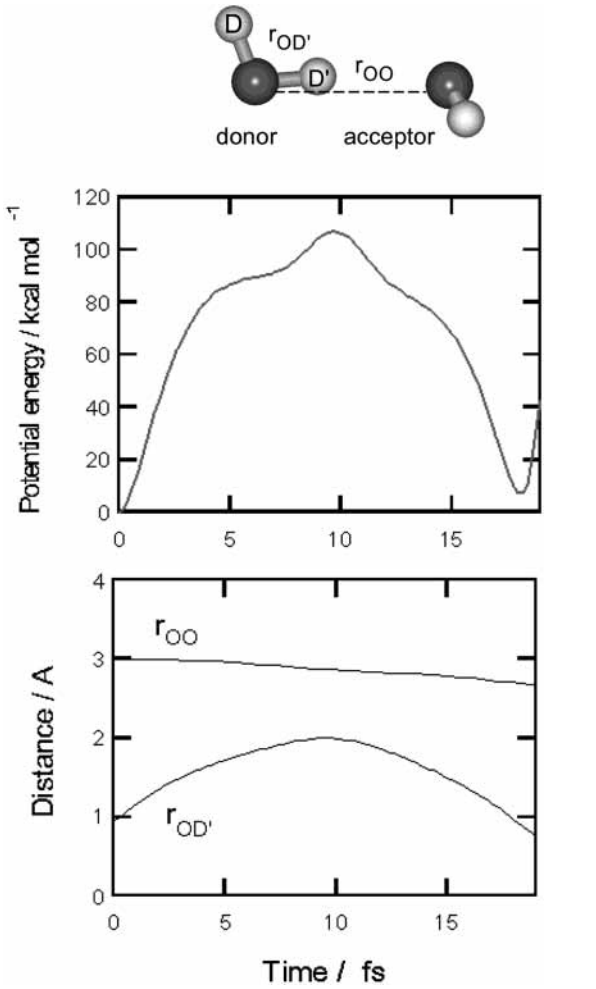

Figure 4. Sample trajectory calculation for the O−D dissociation processes in $(D_2O)_2$. The upper panel shows the potential energy of the reaction. The lower panel shows bond distances vs reaction time. The upper schematic structure of $(D_2O)_2$ indicates the optimized one and the geometrical parameters.

Energy Distribution of the Photofragment Hydrogen Atom from the Water Dimer. In the present work, a direct ab initio trajectory calculation is carried out for the dissociation process of a water dimer in order to estimate how the kinetic energy distribution of the D atom fragment is collisionally relaxed in the dimer.[16,17] Although this calculation has been performed on the ground state potentials and not on the electronically excited potential, the results give an idea about the amount of energy transferred to the acceptor water molecule during the collision process. In the present trajectory calculation, collision energy is initially added as a momentum vector to the D atom of the donor water molecule (denoted by D′ in the dimer structure of Figure 4). The collision energy is chosen as 120 kcal mol^{-1} from the bottom of the potential surface of the donor water, which is 9 kcal mol^{-1} below the dissociation limit, D_0 = 119.8 kcal mol^{-1},[14] because the present calculations are carried out at the Hartree−Fock level (HF/6-311+G(d,p) level) where it is impossible to represent dynamics over the dissociation limit of OD + D′. At time zero, the directions of the momentum vector on the D′ atoms are randomly generated in the ±5.0° range as angles of O−D−O. A total of 30 trajectories are run.

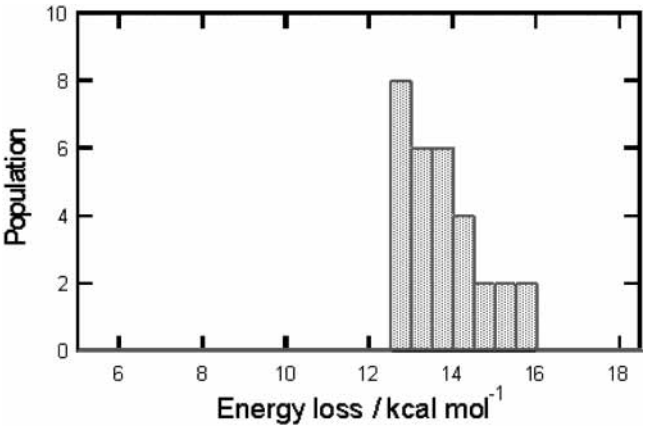

Figure 5. Population of energy loss of the D′ atom of the hydrogen bond donor D′OD, which is caused by one collision with the O atom of the hydrogen bond acceptor D_2O in the water dimer. (See Figure 4.) A total of 30 trajectories are run.

A result for one of the trajectories is given in Figure 4 as a sample, which shows the potential energy change of the reaction system and geometrical parameters. After starting the trajectory, the D′ atom of the parent molecule DOD′ (donor) approaches the O atom of D_2O (acceptor). Then, the D′ atom collides first with the O atom at time 9.8 fs. At time 18.2 fs, the D′ atom collides again with the O atom of DOD′. After this second collision, the D′ atom will depart from the dimer almost on the plane of the parent DOD′ molecule. The distance between the two O atoms is shortened gradually, and the hydrogen bond is retained during the reaction. The potential energy of the system increases as a function of reaction time. The maximum potential energy is calculated to be 106.7 kcal mol^{-1} at the first collision, indicating that 13.3 kcal mol^{-1} is transferred into D_2O, that is, the loss of the translational energy of the fragment D′ atom would be 13.3 kcal mol^{-1} for this sample trajectory. Figure 5 shows the population of the energy loss of the fragment D atom for 30 trajectories, which is induced by the collision to D_2O (acceptor). The population is distributed in the range of 12−16 kcal mol^{-1}. The mean loss energy is 13.6 kcal mol^{-1}. We performed similar trajectory calculations for $(H_2O)_2$ with a collision energy of 120 kcal mol^{-1}. The mean loss energy is 9.7 kcal mol^{-1}. This difference in energy is due to the mass difference between D and H, that is, the lighter H atom retains the higher translational energy.

Discussion

In the following discussion, the D atoms in the water dimer will be referred to as follows: (a) the free D atom refers to any of the three O−D bonds not participating in hydrogen bonding and (b) the hydrogen bond D atom refers to the D atom participating in the hydrogen bond between the two water molecules. Since the hydrogen bond is weak, the dynamics of the free D atom elimination is considered to be a process similar to that from a water monomer. According to Plusquellic et al.[2] the D atom product from the photolysis of the D_2O monomer at 193 nm is translationally hot because the vibrational level of the fragment OD is zero and the mean rotational energy over the three fine structure levels is 200 cm^{-1} (0.6 kcal mol^{-1}).[2] In the case of dimer dissociation, the hydrogen bond D atom should have a different energy distribution from that of the free D atoms because it is "trapped" between the two O atoms and collides with the O atom before it is released from the donor molecule. The lower energy component in Figure 3 corresponds to this type of photofragment, which indicates that 15 kcal mol^{-1} are transferred to the internal energy of OD and D_2O. According to our trajectory calculation, the mean loss energy is 13.6 kcal mol^{-1} with a range of 12−16 kcal mol^{-1}. This calculation reproduces the lower energy distribution of Figure 3. The energy loss is mainly caused by the collision with the O atom of the acceptor water molecule and not with that of the donor water molecule, because the fragmentation of the D′ atom (or the half-collision with the donor water molecule) induces only rotational excitation which is less than 0.6 kcal mol^{-1} according to the reported photodissociation results at 193 nm.[2]

About the distribution of the angular anisotropy parameters shown in the upper panel of Figure 3, this distribution reflects the angular distribution of the hydrogen bond D′ atom. Since the D′ atom interacts strongly with the O atom during the three-body dissociation process, the original speed is relaxed but its fly-away direction is retained in the molecular plane. For the one-photon dissociation of the H_2O monomer in the A^1B_1−X^1A_1 band at 193 nm, Bar et al. reported $\beta_i = -0.44$.[18] The angular anisotropy parameter β_2 strongly depends on the rotational levels of the counter fragment OD after a simple impact parameter model that can be used to calculate the change of β_2 for different rotational levels of OD.[19,20] This model is based on the principle of total angular momentum conservation in the dissociation process. For a distance of R_c between D and OD at which dissociation occurs and an available energy E_{avl} for the dissociation process, the anisotropy parameters for rotationally excited OD products can be calculated using the following formula

$$\beta(N) = A_0\{3N(N+1)h^2/2mR_c^2[E_{avl} - E_{rot}(OD)] - 1\} \quad (5)$$

where A_0 is a factor that accounts for the blurring of anisotropy due to parent rotational excitation. With the use of the theoretical maximum value $\beta_2 = -1$ for the perpendicular transition, the best-fit calculation in the low-energy region gives $R_c = 1.4$−1.7 Å and $E_{avl} = 2.7$−3.5 kcal mol^{-1}. These two values are considered to be fitting parameters in eq 5. The present $R_c = 1.4$−1.7 Å for the dimer is much shorter than 2.2 Å for the vacuum UV photodissociation of the isolated H_2O monomer[18] because the hydrogen bond D fragment is "trapped" in the dimer structure. The small $E_{avl} = 2.4$−3.5 kcal mol^{-1} is due to the energy loss process of the hydrogen bond D atom fragment. The initial part of the curve thus obtained fits the data of Figure 3 well, while mismatching is seen in the region above 5 kcal mol^{-1} because the data are mixed with the background isotropic distribution of the two-photon dissociation of the higher clusters.

Conclusion

In this study we have presented the results of a photofragment imaging experiment for velocity distributions of the D atoms from the photodissociation of the D_2O dimer at 205 nm. Fragment D atoms have slow and fast speed distributions. The angular anisotropy parameters β_2 for the fragment D atoms have negative values. The slow distribution corresponds to the hydrogen-bonding D atom, while the fast one corresponds to the non-hydrogen-bonding D atom. The hydrogen-bonding D atom fragment is translationally relaxed by a collisional process in the dimer, and its dissociation dynamics appears to release the fragments in the plane of the parent water molecule. The loss of the translational energy of the D atom in the collision process is estimated from a direct ab initio trajectory calculation, which is in good agreement with the present experimental results.

Acknowledgment. This work is supported by a Grants-in-Aid from the Ministry of Education, Japan in a priority research

field "Radical Chain Reactions" and by a Grant from the 21st century COE project of Kyoto University.

References and Notes

(1) Chung, C.-Y.; Chew, E. P.; Cheng, B-M.; Bahou, M.; Lee, Y.-P. *Nucl. Instrum. Methods Phys. Res., Sect. A* **2001**, *467*, 1572.

(2) Plusquellic, D. F.; Votava, O.; Nesbitt, D. J. *J. Chem. Phys*. **1997**, *107*, 6123.

(3) Harvey, J. N.; Jung, J. O.; Gerber, R. B. *J. Chem. Phys.* **1998,** *109*, 8747.

(4) Miller, Y.; Fredj, E.; Harvey, J. N.; Gerber, R. B. *J. Phys. Chem.* A **2004**, *108*, 4405.

(5) Goldman, N.; Fellers, R. S.; Brown, M. G.; Braly, L. B.; Keoshian, C. J.; Leforestier, C.; Saykally, R. J. *J. Chem. Phys.* **2002**, *116*, 10148.

(6) Bersohn, R. *Annu. Rev. Phys. Chem.* **2003**, *54*, 1 and references therein.

(7) Zare, R. N. *Mol. Photochem.* **1972**, *4*, 1.

(8) Bush, G. E.; Wilson, K. R. *J. Chem. Phys.* **1972**, *56*, 3626.

(9) Chandler, D. W.; Houston, P. L. *J. Chem. Phys.* **1987**, *87*, 1445.

(10) Eppink, A. T. J. B.; Parker, D. H. *Rev. Sci. Instrum.* **1997**, *68*, 3477.

(11) Sato, Y.; Matsumi, Y.; Kawasaki, M.; Tsukiyama, K.; Bersohn, R. *J. Phys. Chem.* **1995**, *99*, 16307.

(12) Quandt, R.; Wang, X. B.; Min, Z. Y.; Kim, H. L.; Bersohn, R. *J. Phys. Chem. A* **1998**, *102*, 6063.

(13) Zhang, J. Z.; Abramson, E. H.; Imre, D. G. *J. Chem. Phys.* **1991**, *95*, 6536.

(14) Harrich, S. A.; Yang, X.; Hwang, D. W. H.; Lin, J. J.; Yang, X.; Dixon, R. N. *J. Chem. Phys.* **2001**, *114*, 7830.

(15) Frisch, M. J.; Trucks, G. W.; Schlegel, H. B.; Scuseria, G. E.; Robb, M. A.; Cheeseman, J. R.; Zakrzewski, V. G.; Montgomery, J. A., Jr.; Stratmann, R. E.; Burant, J. C.; Dapprich, S.; Millam, J. M.; Daniels, A. D.; Kudin, K. N.; Strain, M. C.; Farkas, O.; Tomasi, J.; Barone, V.; Cossi, M.; Cammi, R.; Mennucci, B.; Pomelli, C.; Adamo, C.; Clifford, S.; Ochterski, J.; Petersson, G. A.; Ayala, P. Y.; Cui, Q.; Morokuma, K.; Malick, D. K.; Rabuck, A. D.; Raghavachari, K.; Foresman, J. B.; Cioslowski, J.; Ortiz, J. V.; Stefanov, B. B.; Liu, G.; Liashenko, A.; Piskorz, P.; Komaromi, I.; Gomperts, R.; Martin, R. L.; Fox, D. J.; Keith, T.; Al-Laham, M. A.; Peng, C. Y.; Nanayakkara, A.; Gonzalez, C.; Challacombe, M.; Gill, P. M. W.; Johnson, B. G.; Chen, W.; Wong, M. W.; Andres, J. L.; Head-Gordon, M.; Replogle, E. S.; Pople, J. A. *Gaussian 98W*, revision A.11.2; Gaussian, Inc.: Pittsburgh, PA, 1998.

(16) Tachikawa, H. *Chem. Phys. Lett.* **2003**, *370*, 188.

(17) Tachikawa, H.; Kawabata, H. *J. Phys. Chem. B* **2003**, *107*, 1113.

(18) Bar, I.; David, D.; Rosenwaks, S. *Chem. Phys.* **1994**, *187*, 21.

(19) Hwang, D. W.; Yang, X. F.; Harich, S.; Lin, J. J.; Yang, X. *J. Chem. Phys.* **1999**, *110*, 4123.

(20) Mordaunt, D. H.; Ashfold, M. N. R.; Dixon, R. N. *J. Chem. Phys.* **1996**, *104*, 6460.